Nondegenerate two-photon optical bistability in a Fabry-Perot cavity filled with large-permanent-dipole molecules

T. Kobayashi, N. C. Kothari, and H. Uchiki
Department of Physics, University of Tokyo, 3-1 Hongo, 7-chome, Bunkyo-ku, Tokyo 113, Japan
(Received 15 September 1983)

A semiclassical theoretical model is described under the plane-wave and mean-field approximations on the transmission characteristics of a system of two-level atoms with large permanent dipole moments contained in a Fabry-Perot cavity and driven by two coherent two-photon resonant fields. In the steady-state situation, the coupled field equations are solved by eliminating one of the field variables to obtain the state equation. This state equation is numerically analyzed in detail, thus providing the regions on two-dimensional maps corresponding to one, three, and five stationary states of the system. The linear stability analysis is also carried out for the case when the length of the cavity is such that the medium-relaxation times are much shorter than the cavity-photon life times for both the waves. The simple stability criterion that the negative-slope regions of the transmission curves are unstable holds, but only the lowest positive-slope branches show stability in all of the cases we tested numerically.

I. INTRODUCTION

The phenomenon of optical bistability, in which under appropriate conditions the light intensity transmitting nonlinear interferometer exhibits hysteresis cycle, has been proposed and observed experimentally.[1–5] Great deal of attention has been paid by a number of scientific groups on this subject due to its potential device applications to optical computers and transistors. Also, from the theoretical viewpoint this phenomenon constitutes an interesting example of a system driven far from equilibrium which exhibits a first-order phase transition. A number of different optical systems have been suggested which could exhibit bistable behavior under certain excitation conditions and some sets of the system parameters. Walls *et al.*[6] have reviewed the bistable systems in nonlinear optics, and irradiated Josephson junctions have been considered by Agarwal and Shenoy.[7] A paper by Toyozawa[8] predicts bistability in exciton-photon interaction, whereas Hanamura's theoretical model[9] on CuCl provides a possible picosecond switching time by considering an off-resonant excitation under the purely virtual dispersive process which has the response time of the order of transverse relaxation time, in a micrometer size cavity.

It has been shown[10–14] that a two-photon resonant system placed inside the cavity can also display optical bistability or multistability under certain circumstances due to the interaction of two fields at different frequencies with each other. The degenerate two-photon system is also shown to exhibit tristable features.[15,16] The two-photon dispersive optical bistability in rubidium vapor was observed experimentally by Giacobino *et al.*[17] The effect of Stark shift on two-photon tristability is discussed by Parigger *et al.*,[18] and possibilities of self-pulsing, period doubling, and optical chaos have been discussed in Ref. 19.

Recently, we have described a model[20] on degenerate two-photon bistability in a Fabry-Perot cavity filled with molecules having large permanent dipole moments. It was shown that for a large-permanent-dipole molecule, the two-photon optical bistability can result in a submicrometer-sized Fabry-Perot cavity. The importance of the analysis was stressed in its possible application in constructing optical bistable devices of submicrometer dimensions. In this paper we discuss the nondegenerate case, and obtain the corresponding state equation for steady-state conditions treating one of the beam intensities as a controlling parameter. The state equation is analyzed numerically to obtain different regions corresponding to one, three, and five stationary states of the system. Linear stability analysis is also carried out for some simplifying conditions.

II. THEORY

We consider a system of N molecules with two levels $|a\rangle$ (ground level) and $|b\rangle$ (excited level) which are contained in the Fabry-Perot cavity. The excited level $|b\rangle$ is connected with the ground level $|a\rangle$ by electric dipolar interaction $-\mu_{ba}\tilde{E}(t)$ with internal radiation field $\tilde{E}(t)$, composed of two different frequencies. The levels $|a\rangle$ and $|b\rangle$ have mixed parities with permanent dipole moments μ_{aa} and μ_{bb}. The two-photon transition between two levels is allowed if at least either one of the two levels has the mixed parity, in which case the diagonal element of the dipole is nonvanishing[21] (permanent dipole moment). The Hamiltonian of the system may be written as follows:

$$\begin{aligned} H_{ba} &= -\tfrac{1}{2}\mu_{ba}(E_1 e^{-i\omega_1 t}+E_2 e^{-i\omega_2 t}+\text{c.c.})=H_{ab}^{*}\ , \\ H_{bb} &= -\tfrac{1}{2}\mu_{bb}(E_1 e^{-i\omega_1 t}+E_2 e^{-i\omega_2 t}+\text{c.c.})\ , \\ H_{aa} &= -\tfrac{1}{2}\mu_{aa}(E_1 e^{-i\omega_1 t}+E_2 e^{-i\omega_2 t}+\text{c.c.})\ . \end{aligned} \tag{1}$$

Here ω_1 and ω_2 are frequencies of two different incident waves, E_1 and E_2 being their slowly varying envelopes. The density matrix elements obey the following equations of motion in the mean-field approximations:

$$i\hbar\dot{\rho}_{ba} = -H_{ba}\rho_D + \hbar(\omega_{ba} - i/T_2)\rho_{ba} + (H_{bb} - H_{aa})\rho_{ba} , \tag{2a}$$

$$i\hbar\dot{\rho}_D = 2(H_{ba}\rho_{ab} - \rho_{ba}H_{ab}) - i\hbar T_1^{-1}(\rho_D - \rho_D^{(0)}) , \tag{2b}$$

$$\rho_D = \rho_{bb} - \rho_{aa} , \tag{2c}$$

where ω_{ba} is the energy gap between the two levels $|a\rangle$ and $|b\rangle$, T_2 is the transverse relaxation time, T_1 is the longitudinal relaxation time, and $\rho_D^{(0)}$ is the equilibrium population difference between the two levels in the absence of a radiation field. The temperature-dependent term in Eq. (2b) has been ignored.[22] In what follows, we shall assume T_1^{-1}, $T_2^{-1} \ll \omega_1, \omega_2$. For the incident field $\frac{1}{2}[(E_{10}e^{-i\omega_1 t} + E_{20}e^{-i\omega_2 t})e^{ikr} + \text{c.c.}]$, the envelope functions $E_j(t)$, $j=1,2$ relax to $E_{j0}/\sqrt{T}$ in the empty cavity and the effect of the cavity is described by

$$\gamma_j = \frac{cT_{0j}}{2Ln_j} + i\frac{c\theta_j}{2Ln_j}, \quad \theta_j = 2kL - 2m_j\pi \tag{3}$$

where T_{0j} are the transmittance coefficients of the mirrors for two waves $j=1$ and 2, m_j are integers, c is the light velocity in vacuum, and n_j are the linear refractive indices of the medium for the two waves. For simplicity, $E_{j0}/\sqrt{T}$ are replaced by E_{j0}. Then the equations of motion for field amplitudes $E_j(t)$ may be written as

$$\dot{E}_j(t) = -\gamma_j[E_j(t) - E_{j0}] - i\frac{2\pi\omega_j N}{V}[\mu_{ba}^*\hat{\rho}_{ba}(\omega_j) + \mu_{aa}\hat{\rho}_{aa}(\omega_j) + \mu_{bb}\hat{\rho}_{bb}(\omega_j)], \tag{4}$$

where $\hat{\rho}_{ba}$, $\hat{\rho}_{aa}$, and $\hat{\rho}_{bb}$ are the amplitudes of the terms oscillating with frequencies ω_j in ρ_{ba}, ρ_{aa}, and ρ_{bb}, respectively. We shall be interested in the transmission characteristics of the system under the steady-state conditions. Hence the stationary solutions of Eqs. (2) and (4) would constitute the basic mathematical analysis. As was done in the degenerate case,[20] we follow the perturbation approach to the problem and expand ρ_{ba} and ρ_D as follows:

$$\hat{\rho}_{ba}(\omega_j) \simeq \hat{\rho}_{ba}^{(1)}(\omega_j) + \hat{\rho}_{ba}^{(3)}(\omega_j) ,$$
$$\hat{\rho}_D(\omega_j) \simeq \hat{\rho}_D^{(3)}(\omega_j) . \tag{5}$$

For the two-photon nondegenerate resonant condition ($\omega_{ba} \approx \omega_1 + \omega_2$, and $|2\omega_j - \omega_{ba}| \gg |\omega_1 + \omega_2 - \omega_{ba}|$), and for $\mu_0^2/\mu_{ba}^2 \gg 1$ where $\mu_0 = (\mu_{aa} - \mu_{bb})/2$, we have, for the steady-state situation,

$$\hat{\rho}_{ba}^{(1)}(\omega_j) = -i\hbar^{-1}\frac{\mu_{ba}}{2}E_j\rho_D^{(0)}\frac{1}{D_j} , \tag{6}$$

$$\hat{\rho}_{ba}^{(3)}(\omega_j) = i\hbar^{-3}\frac{\mu_{ba}}{2}\mu_0^2\rho_D^{(0)} \times \left[\frac{1}{D_j D_0}\left(\frac{1}{D_j} + \frac{1}{D_{3-j}}\right)E_j|E_{3-j}|^2\right] , \tag{7}$$

$$\hat{\rho}_D^{(3)}(\omega_j) = i\hbar^{-3}\frac{\mu_0}{2}|\mu_{ba}|^2\rho_D^{(0)} \times \left[\frac{1}{D_{1j}D_0}\left(\frac{1}{D_j} + \frac{1}{D_{3-j}}\right)E_j|E_{3-j}|^2\right] , \tag{8}$$

with

$$D_j = T_2^{-1} + i(\omega_{ba} - \omega_j) ,$$
$$D_0 = T_2^{-1} + i[\omega_{ba} - (\omega_1 + \omega_2)] ,$$
$$D_{1j} = T_1^{-1} - i\omega_j .$$

When Eqs. (5)—(8) are substituted in Eqs. (4), we have the following equations for steady-state conditions $[\dot{E}_j(t) = 0]$:

$$E_{j0} = (1 + A_j)E_j(t) + B_jE_j(t)|E_{3-j}(t)|^2, \quad j = 1,2 \tag{9}$$

where

$$A_j = \frac{\pi\omega_j N}{V\gamma_j}\frac{|\mu_{ba}|^2}{\hbar D_j}\rho_D^{(0)} \tag{10}$$

and

$$B_j = \frac{\pi\omega_j N}{V\gamma_j}\frac{|\mu_{ba}|^2\mu_0^2}{\hbar^3 D_0}\left(\frac{1}{D_1} + \frac{1}{D_2}\right)\left(\frac{1}{D_{1j}} - \frac{1}{D_j}\right)\rho_D^{(0)} . \tag{11}$$

If we write Eqs. (9) for $j=1$ and 2 separately, we have

$$E_{10} = (1 + A_1)E_1(t) + B_1E_1(t)|E_2(t)|^2 , \tag{12a}$$

$$E_{20} = (1 + A_2)E_2(t) + B_2E_2(t)|E_1(t)|^2 . \tag{12b}$$

From Eqs. (12), we eliminate $|E_2(t)|^2$, and obtain the state equation for $|E_{10}|^2$ in terms of $|E_1(t)|^2$ and $|E_{20}|^2$ as follows:

$$y_1 = x_1\left[1 - \frac{\delta y_2}{1 - \delta x_1 + x_1^2} + \frac{ay_2^2}{(1 - \delta x_1 + x_1^2)^2}\right] , \tag{13}$$

where we have normalized the field powers by defining

$$y_1 = |E_{10}|^2\frac{|B_2|}{|A_1 + 1|^2|A_2 + 1|} , \tag{14}$$

$$x_1 = |E_1|^2\frac{|B_2|}{|A_2 + 1|} , \tag{15}$$

$$y_2 = |E_{20}|^2\frac{|B_2|}{|A_1 + 1|^2|A_2 + 1|} \times \left[\frac{\mathrm{Re}[(A_1 + 1)B_1^*]}{\mathrm{Re}[(A_2 + 1)B_2^*]}\right] , \tag{16}$$

$$\delta = -\frac{2\,\mathrm{Re}[(A_2^* + 1)B_2]}{|(A_2^* + 1)B_2|} , \tag{17}$$

and

$$a = \left[\frac{\mathrm{Re}[(A_2 + 1)B_2^*]}{\mathrm{Re}[(A_1 + 1)B_1^*]}\right]^2\left[\frac{|B_1|^2|A_1 + 1|^2}{|B_2|^2|A_2 + 1|^2}\right] . \tag{18}$$

Here, the parameter δ plays a similar role as that of the

parameter c in the Bonifacio-Lugiato model[3] of mean-field absorptive optical bistability in a ring cavity. The parameter a may be called the nondegeneracy parameter, as $a \neq 1$ corresponds to the nondegenerate case where the cavity is driven by two distinct coherent fields, whereas $a=1$ produces degeneracy in the frequencies of the driving fields.

For two-photon resonant condition $\omega_1+\omega_2=\omega_{ba}$, a in expression (18) can be written in terms of system parameters as follows:

$$a=\frac{|\gamma_2|^2}{|\gamma_1|^2}\left[\frac{\left[\frac{c}{2L}\right]^2+\left[\frac{\pi\omega_1 n_1 N}{VT_{01}}\frac{|\mu_{ba}|^2\rho_D^{(0)}}{\hbar\omega_2}-\frac{c\theta_1}{2LT_{01}}\right]^2}{\left[\frac{c}{2L}\right]^2+\left[\frac{\pi\omega_2 n_2 N}{VT_{02}}\frac{|\mu_{ba}|^2\rho_D^{(0)}}{\hbar\omega_1}-\frac{c\theta_2}{2LT_{02}}\right]^2}\right] . \tag{19}$$

It can be easily verified that for the two-photon resonant condition and for $\mu_0^2/\mu_{ba}^2 \gg 1$, we have

$$(A_j^*+1)B_j+(A_j+1)B_j^*<0, \quad j=1,2 \tag{20}$$

which imply that $\delta>0$. Also, the straightforward observation of Eq. (13) suggests that, for $a<1$ we must have $\delta<2\sqrt{a}$ and for $a>1$ we must have $\delta<2$ in order to have y_1 positive finite. The state equation (13) is the fifth-order polynomial equation for the internal field power $|E_1|^2$ in terms of input field powers $|E_{10}|^2$, $|E_{20}|^2$, and other system parameters. It has five roots, and hence displays either one, three, or five stationary branches depending on which whether it has one, three, or five positive real roots, respectively. The degenerate case results [$\omega_1=\omega_2=\omega$ and $E_1/2=E_2/2=E$ in Eqs. (1)] of Ref. 20 can be obtained by substituting $a=1$ with $y_2=y_1=y$ and $x_1=x$ in Eq. (13) and taking $A_1=A_2=A$ and $B_1/2=B_2/2=B$ in Eqs. (10) and (11).

III. NUMERICAL CALCULATIONS

In this section we present a detailed numerical analysis in order to investigate the different stationary regions corresponding to one, three, and five stationary branches of the state equation (13) between the input-output variables y_1 and x_1. The numerical calculations have been performed with many sets of the parameters a, δ, and y_2. To obtain the maps of different regions on the y_2-δ plane, the following method was used.

We express the state equation (13) in the form of a fifth-order polynomial equation for x_1 as

$$x_1^5-(2\delta+y_1)x_1^4+(2-\delta y_2+\delta^2+2\delta y_1)x_1^3+(\delta^2 y_2-2\delta-2y_1-\delta^2 y_1)x_1^2+(ay_2^2-\delta y_2+2\delta y_1+1)x_1-y_1=0 . \tag{21}$$

We make a simple transformation by replacing x_1 with $x_1+\delta/2$ for mathematical convenience, and obtain the following equation:

$$x_1^5+\left[\frac{\delta}{2}-y_1\right]x_1^4+(2\nu-\delta y_2)x_1^3+\left[\frac{\delta(2\nu-\delta y_2)}{2}-2\nu y_1\right]x_1^2+(\nu^2-\delta\nu y_2+ay_2^2)x_1+\left[\frac{\delta}{2}(\nu^2-\delta\nu y_2+ay_2^2)-\nu^2 y_1\right]=0 , \tag{22a}$$

where

$$\nu=1-(\delta^2/4) . \tag{22b}$$

The triply degenerate roots of Eq. (22a), say $\alpha_1=\alpha_2=\alpha_3=\alpha$, correspond to the boundary between the regions of one, three, and five stationary branches in the y_2-δ plane, since slight deviations from the relationship $\alpha_1=\alpha_2=\alpha_3$ give rise to three- or five- branch behavior of the system from either one- or three-branch behavior. Hence to obtain the different regions, we compare the coefficients of Eq. (22a) with the coefficients of the following equation:

$$(x_1-\alpha)^3(x_1^2-\beta x_1+\eta)=0 . \tag{23}$$

The five coupled equations thus obtained in terms of α, β, η, a, δ, y_1, and y_2 can be shown to reduce into the following two equations by simple but lengthy algebraic manipulations, where the parameters β, η, and y_1 are totally eliminated:

$$a(\nu+3\alpha^2)y_2^2-(\delta\nu^2+3\alpha^4\delta+2\alpha^3\delta^2)y_2+(\nu+\alpha^2)^2(\nu-5\alpha^2)=0 , \tag{24}$$

$$\delta y_2=\frac{2(\nu+\alpha^2)^2[\nu(6\alpha+\delta)-6\alpha^3-5\alpha^2\delta]}{(\nu-3\alpha^2)[\nu(6\alpha+\delta)-2\alpha^3-3\alpha^2\delta]+16\alpha^3} . \tag{25}$$

By changing α from 0 to 1.1, Eqs. (24) and (25) were solved numerically to obtain y_2 and δ for different values of the parameter a. For $\alpha>1.1$, no (y_2,δ) pair was obtained for the values of the parameter a chosen. Each (y_2,δ) pair corresponds to a point on the y_2-δ map, which falls either on the curve or on the line. In Fig. 1, we show several y_2-δ maps for the different values of a. The mean-

ingful region of the y_2-δ plane is restricted by the condition $y_2 \geq 0$ and $\delta < 2$ for $a > 1$ or $\delta < 2\sqrt{a}$ for $a < 1$, as mentioned in Sec. II. The regions denoted in Fig. 1 by I, II, and III show the regions corresponding to one, three, and five stationary states of the system, respectively. The region III has two different types of transmission characteristics. In type one, the first maximum value $y_{11}^{\max}$ is smaller than the second minimum value $y_{12}^{\min}$, whereas in type two, $y_{11}^{\max}$ is larger than $y_{12}^{\min}$ (see Fig. 2). The transmission curves of types one and two exhibit similar characteristics as those of the double bistability and tristability curves, respectively, obtained by Fuli.[23]

In Figs. 3(a)—3(d), we show several input-output (y_1-x_1) plots for a different set of parameters a, δ, and y_2. It may be noticed that one has an active control on the switching energies by varying the field intensity of the second beam (y_2), as the transmission curves differ significantly from each other when y_2 is changed.

Here, one should note that to obtain curves in Figs. 1—3, we have used the values of x_j up to about 2 in Eq. (13). We numerically estimated the contributions of fifth and higher-order nonlinear terms for these values of x_j (field intensities) and the other parameters chosen in this paper and in Ref. 20. We found that these contributions can be neglected in comparison with the third-order nonlinear term for two-photon resonant conditions. Hence Eqs. (12) are accurate for the treatment presented in this paper.

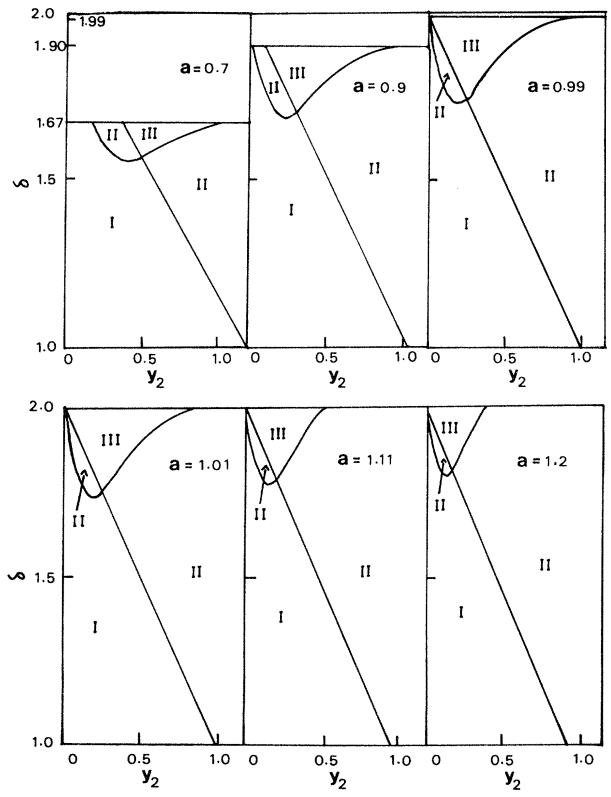

FIG. 1. y_2-δ maps for six different values of the parameter a. The regions denoted by I, II, and III show the regions corresponding to one, three, and five stationary states of the system, respectively. The values of $\delta = 1.67$, 1.90, and 1.99 are the $\delta = 2\sqrt{a}$ values for $a = 0.7$, 0.9, and 0.99, respectively.

IV. LINEAR STABILITY ANALYSIS

In this section we perform the linear stability analysis of the stationary solutions of the state equation (13). In its most general form a linear stability analysis is quite complicated, and hence we simplify the problem by imposing some restrictions: (i) We consider the case when $T_1, T_2 \ll \gamma_1^{-1}, \gamma_2^{-1}$. Thus we need to consider only the field equations. (ii) We assume perfect cavity and atomic tuning. This means that B_1 and B_2 are real (negative) quantities, whereas A_1 and A_2 are purely imaginary quantities. (iii) We take $\gamma_1 = \gamma_2 = \gamma$ and define $\tau = \gamma t$. The two field equations for E_1 and E_2 are given as

$$\dot{E}_1 = \gamma_1 E_{10} - \gamma_1(1 + A_1)E_1 - \gamma_1 B_1 E_1 |E_2|^2 , \tag{26a}$$

$$\dot{E}_2 = \gamma_2 E_{20} - \gamma_2(1 + A_2)E_2 - \gamma_2 B_2 E_2 |E_1|^2 . \tag{26b}$$

With $\gamma_1 = \gamma_2 = \gamma$ and $\tau = \gamma t$, Eqs. (26a) and (26b) can be written as

$$\frac{d}{d\tau}|E_1|^2 = 2|E_{10}||E_1|\cos\phi_1 - 2|E_1|^2 - 2B_1|E_1|^2|E_2|^2 , \tag{27a}$$

$$\frac{d\phi_1}{d\tau} + |A_1| = -\frac{|E_{10}|}{|E_1|}\sin\phi_1 , \tag{27b}$$

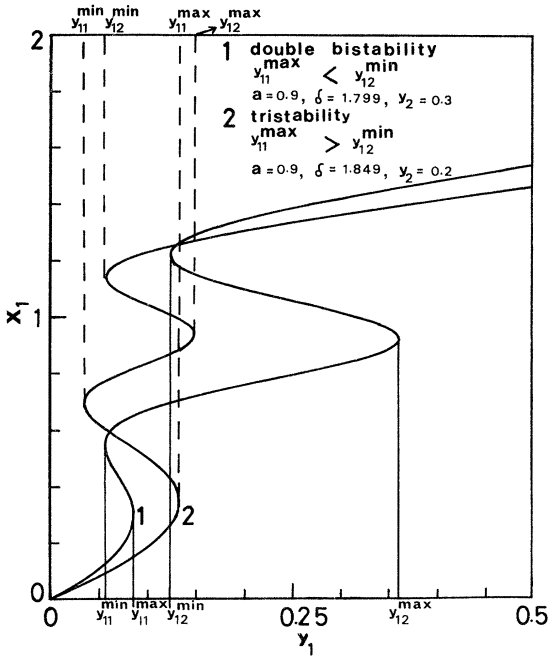

FIG. 2. x_1-y_1 plots showing five stationary states corresponding to region III of Fig. 1 for $a = 0.9$. Curve 1 is of type one, and is similar to the double bistability curves of Ref. 23, whereas curve 2 is of type two, and is similar to the tristability curves of the same reference (see the text for the meanings of types one and two characteristics).

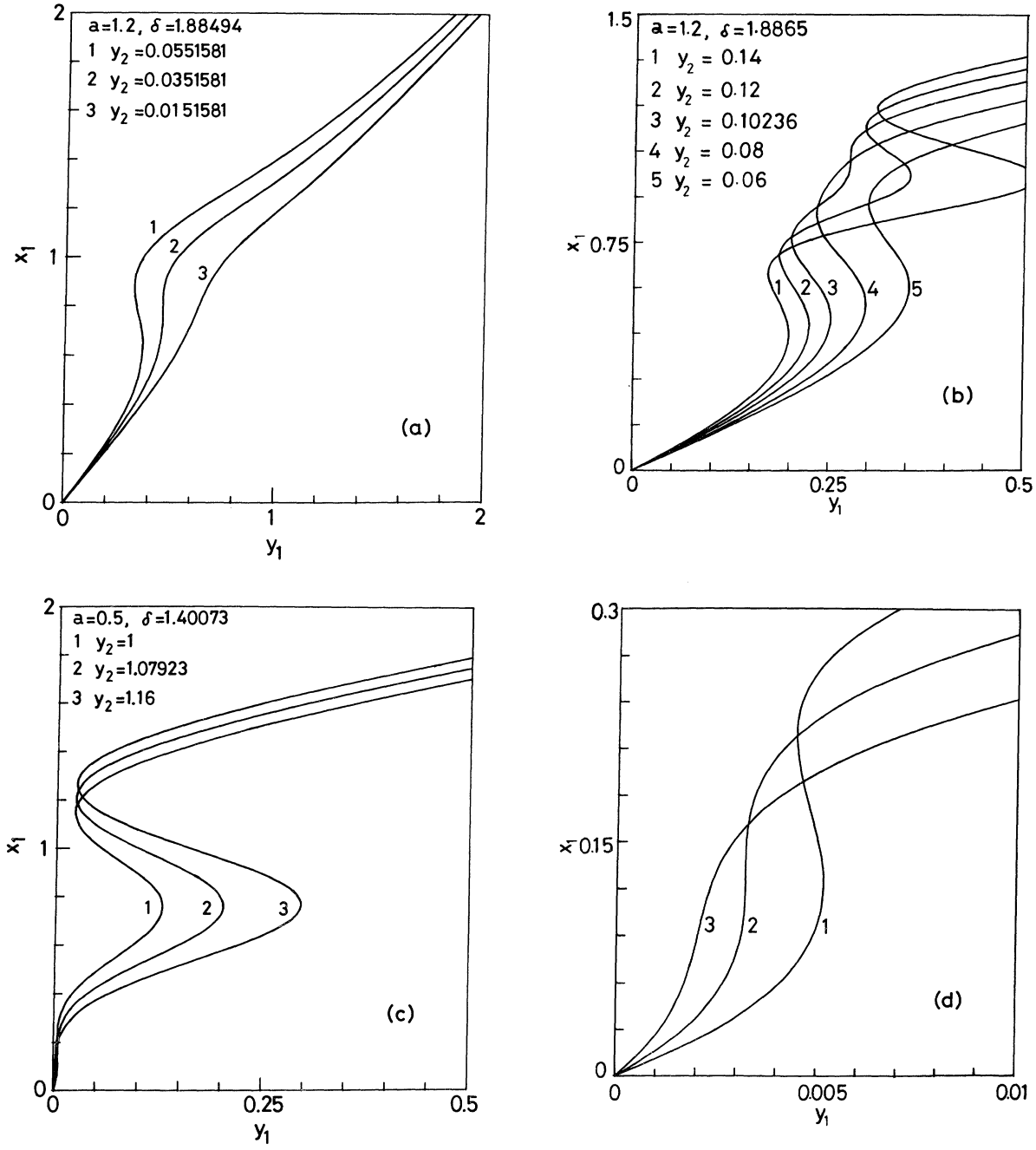

FIG. 3. x_1-y_1 plots for different set of parameters a, δ, and y_2. (a) Curve 1 corresponds to three stationary states of the system, whereas curves 2 and 3 show the single stationary state. (b) Curves 1 and 2 correspond to five stationary states of the system (type one; see the text). They are similar to the double bistability curves obtained in Ref. 23 . Curves 3, 4, and 5 show three stationary states of the system. (c) Curve 1 corresponds to five stationary states of the system. The lower two stationary states are not resolved. The curves 2 and 3 show three stationary states. The lower portions of all the curves are expanded in (d). (d) Expansion of the lower portion of (c).

$$\frac{d}{d\tau}|E_2|^2=2|E_{20}||E_2|\cos\phi_2-2|E_2|^2 -2B_2|E_1|^2|E_2|^2, \tag{27c}$$

$$\frac{d\phi_2}{d\tau}+|A_2|=-\frac{|E_{20}|}{|E_2|}\sin\phi_2, \tag{27d}$$

where $E_1=|E_1|e^{i\phi_1}$, $E_2=|E_2|e^{i\phi_2}$, and the input fields E_{10} and E_{20} are assumed to be real. Here, we need to define x_2 as follows:

$$x_2=|E_2|^2\frac{|B_1|}{|A_2+1|}. \tag{28}$$

With assumption (ii) kept in mind, we obtain the follow-

ing expressions for y_1, x_1, y_2, x_2, δ, and a, which are already defined in Eqs. (14)—(18) and (28):

$$y_1 = |E_{10}|^2 \frac{|B_2|}{(1+|A_1|^2)(1+|A_2|^2)^{1/2}}, \tag{29}$$

$$x_1 = |E_1|^2 \frac{|B_2|}{(1+|A_2|^2)^{1/2}}, \tag{30}$$

$$y_2 = |E_{20}|^2 \frac{|B_1|}{(1+|A_1|^2)(1+|A_2|^2)^{1/2}}, \tag{31}$$

$$x_2 = |E_2|^2 \frac{|B_1|}{(1+|A_2|^2)^{1/2}}, \tag{32}$$

$$a = \frac{1+|A_1|^2}{1+|A_2|^2}, \tag{33}$$

and

$$\delta = \frac{2}{(1+|A_2|^2)^{1/2}}. \tag{34}$$

Using the above normalizing parameters, one can easily obtain the following equations:

$$\frac{dx_1}{d\tau} = \frac{4}{\delta}(ax_1y_1)^{1/2}\cos\phi_1 - 2x_1 + \frac{4}{\delta}x_1x_2, \tag{35}$$

$$\frac{d\phi_1}{d\tau} = -\left[\frac{4a}{\delta^2}-1\right]^{1/2} - \frac{2}{\delta}\left[\frac{ay_1}{x_1}\right]^{1/2}\sin\phi_1, \tag{36}$$

$$\frac{dx_2}{d\tau} = \frac{4}{\delta}(ax_2y_2)^{1/2}\cos\phi_2 - 2x_2 + \frac{4}{\delta}x_1x_2, \tag{37}$$

$$\frac{d\phi_2}{d\tau} = -\left[\frac{4}{\delta^2}-1\right]^{1/2} - \frac{2}{\delta}\left[\frac{ay_2}{x_2}\right]^{1/2}\sin\phi_2. \tag{38}$$

Since B_1 and B_2 are real negative for perfect atomic and cavity tuning, the last terms in Eqs. (35) and (37) have the change in sign. Under the steady-state conditions, the state equation (13) can be very easily recovered after eliminating x_2. It can be shown that for steady-state conditions, the variable x_2 is given as

$$x_2 = \frac{ay_2}{1-\delta x_1+x_1^2}. \tag{39}$$

Now, we carry out the linear stability analysis of Eqs. (35)—(38). We assume the following solutions for these equations:

$$x_j = x_j^s + \Delta x_j, \quad \phi_j = \phi_j^s + \Delta\phi_j, \quad j=1,2 \tag{40}$$

where $|\Delta x_j| \ll x_j^s$, $|\Delta\phi_j| \ll |\phi_j^s|$, and x_j^s and ϕ_j^s are the steady-state values of x_j and ϕ_j, respectively. Substituting the solutions (40) into Eqs. (35)—(38), and linearizing the equations, we obtain

$$\frac{d}{d\tau}\begin{bmatrix}\Delta x_1\\ \Delta\phi_1\\ \Delta x_2\\ \Delta\phi_2\end{bmatrix} = \begin{bmatrix} P_1 & Q_1 & \frac{4}{\delta}x_1^s & 0\\ R_1 & S_1 & 0 & 0\\ \frac{4}{\delta}x_2^s & 0 & P_2 & Q_2\\ 0 & 0 & R_2 & S_2\end{bmatrix}\begin{bmatrix}\Delta x_1\\ \Delta\phi_1\\ \Delta x_2\\ \Delta\phi_2\end{bmatrix}, \tag{41}$$

where

$$P_j = \frac{2}{\delta}\left[\frac{ay_j}{x_j^s}\right]^{1/2}\cos\phi_j^s - 2 + \frac{4}{\delta}x_{3-j}^s, \tag{42}$$

$$Q_j = -\frac{4}{\delta}(ay_jx_j^s)^{1/2}\sin\phi_j^s, \tag{43}$$

$$R_j = \frac{1}{\delta}\left[\frac{ay_j}{x_j^s}\right]^{1/2}\frac{1}{x_j^s}\sin\phi_j^s, \tag{44}$$

$$S_j = -\frac{2}{\delta}\left[\frac{ay_j}{x_j^s}\right]^{1/2}\cos\phi_j^s. \tag{45}$$

The steady-state values of ϕ_j^s can be written as

$$\sin\phi_1^s = -\left[\frac{x_1^s}{y_1}\left[1-\frac{\delta^2}{4a}\right]\right]^{1/2}, \tag{46a}$$

$$\cos\phi_1^s = (\delta/2 - x_2^s)\left[\frac{x_1^s}{ay_1}\right]^{1/2}, \tag{46b}$$

$$\sin\phi_2^s = -\left[\frac{x_2^s}{ay_2}\left[1-\frac{\delta^2}{4}\right]\right]^{1/2}, \tag{46c}$$

$$\cos\phi_2^s = (\delta/2 - x_1^s)\left[\frac{x_2^s}{ay_2}\right]^{1/2}. \tag{46d}$$

Applying the extended Routh-Hurwitz criterion, we obtain the following stability conditions:

$$M_1 > 0, \tag{47a}$$

$$M_2 > M_3/M_1, \tag{47b}$$

$$M_3 > M_1^2M_4/(M_1M_2 - M_3), \tag{47c}$$

$$M_4 > 0, \tag{47d}$$

where

$$M_1 = 4\left[1-\frac{1}{\delta}(x_1^s+x_2^s)\right], \tag{48a}$$

$$M_2 = \frac{4a}{\delta^2}\left[\frac{y_1}{x_1^s}+\frac{y_2}{x_2^s}\right] + 4\left[1-\frac{2}{\delta}(x_1^s+x_2^s)\right], \tag{48b}$$

$$M_3 = \left[\frac{16}{\delta^2}x_1^sx_2^s - \frac{8a}{\delta^2}\frac{y_1}{x_1^s}\right]\left[\frac{2x_1^s}{\delta}-1\right] + \left[\frac{16}{\delta^2}x_1^sx_2^s - \frac{8a}{\delta^2}\frac{y_2}{x_2^s}\right]\left[\frac{2x_2^s}{\delta}-1\right], \tag{48c}$$

$$M_4 = \frac{16}{\delta^4}\left[a^2\frac{y_1y_2}{x_1^sx_2^s} - x_1^sx_2^s(2x_1^s-\delta)(2x_2^s-\delta)\right]. \tag{48d}$$

For all possible steady-state solutions of Eq. (13), one should test conditions (47) to determine the stability of the stationary branches. It can be verified that the condition (47d) is equivalent to $(dy_1/dx_1^s) > 0$, which explains that the negative slope regions of the steady-state transmission curves are unstable. We have tested the conditions (47) numerically for many sets of the parameters a, δ, and y_2. The results suggest that only the lowest positive differen-

tial gain branches are stable in all the cases when Eq. (13) exhibits bistable or tristable behavior. This means that possibly the best situations may occur (the higher positive differential gain branches also showing stability) when the cavity size is of the order of a micrometer to a submicrometer dimension. In such cases, one should test the stability of diffferent branches by developing proper stability criterion for the case when $T_1, T_2, \gg \gamma_1^{-1}, \gamma_2^{-1}$.

V. DISCUSSION AND CONCLUSIONS

In the present paper we have shown that a Fabry-Perot cavity filled with molecules having large permanent dipole moments and driven by two distinct coherent two-photon resonant fields can exhibit bistable behavior. Earlier, we had described the degenerate case,[20] and shown that for a large permanent dipole molecule, the two-photon optical bistability can result in a submicrometer-sized Fabry-Perot cavity. We have also proposed some class of materials, mainly organic and polymeric crystals and films, which can have potential nonlinear device applications. In these organic and polymeric crystals, the high values of $\chi^{(3)}$ arise from delocalized conjugated π bonds. Some of the specific examples[20] of these organic and polymeric class of materials with large permanent dipole moments are[24] (1) 4-dimethylamino-4'-cyanostilbene (DCS) with $\mu_{aa}=6.1$ D and $\mu_{bb}=29$ D; (2) 4-dimethylamino-4'-nitrostilbene (DNS) with $\mu_{aa}=7.6$ D and $\mu_{bb}=32$ D; (3) 2-amino-7-nitrofluorene (ANF) with $\mu_{aa}=7$ D and $\mu_{bb}=25$ D. With proper design and choosing the proper group of organic and polymeric thin films of submicrometer dimension, switching times of the picosecond order may be possible because of large electronic contributions to nonlinearities in the case of molecules having short longitudinal relaxation time T_1 of the picosecond order, and because of the submicrometer size of the cavity. In the nondegenerate case, the stability analysis carried out for the case when $T_1, T_2 \ll \gamma_1^{-1}, \gamma_2^{-1}$ suggests that higher positive slope branches are unstable, thus the system cannot be used as a bistable device when the cavity size is large enough such that the above condition is satisfied. For a cavity size of the order of a micrometer to a submicrometer dimension, one is within the range such that $T_1, T_2 \gg \gamma_1^{-1}, \gamma_2^{-1}$. In such cases, one should test the stability of different branches by developing proper stability criterion. The active control on the switching energies by varying the field intensity of the second beam is evident from the numerical analysis presented in the paper. The detailed calculations on minimum holding power density are not given in the present analysis, but few MW/cm^2 power densities[20] would be required to experimentally observe the predicted bistability.

ACKNOWLEDGMENTS

The authors thank Professor E. Hanamura for valuable discussion. This work was supported in part by a Grant-in-Aid for Scientific Research from the Ministry of Education, Science and Culture of Japan, and in part by the Kajima Foundation's Research Grant.

[1]H. Seidal, U. S. Patent No. 3610731 (1969); S. L. McCall, Phys. Rev. A 9, 1515 (1974).
[2]H. M. Gibbs, S. L. McCall, and T. N. C. Venkatesan, Phys. Rev. Lett. 36, 1135 (1976).
[3]R. Bonifacio and L. A. Lugiato, Opt. Commun. 19, 172 (1976); Phys. Rev. A 18, 1129 (1978); Lett. Nuovo Cimento 21, 517 (1978).
[4]F. S. Felber and J. H. Marburger, Appl. Phys. Lett. 28, 731 (1976); J. H. Marburger and F. S. Felber, Phys. Rev. A 17, 335 (1978).
[5]G. P. Agrawal and H. J. Carmichael, Phys. Rev. A 19, 2074 (1979).
[6]D. F. Walls, P. D. Drummond, and K. J. McNeil, in *Optical Bistability,* edited by C. M. Bowden, M. Ciftan, and H. R. Robl (Plenum, New York, 1981).
[7]G. S. Agarwal and S. R. Shenoy, in *Optical Bistability,* edited by C. M. Bowden, M. Ciftan, and H. R. Robl (Plenum, New York, 1981).
[8]Y. Toyozawa, Solid State Commun. 28, 533 (1978).
[9]E. Hanamura, Solid State Commun. 38, 939 (1981).
[10]F. T. Arecchi and A. Politi, Lett. Nuovo Cimento 23, 65 (1978).
[11]J. A. Hermann and B. V. Thompson, Phys. Lett. 79A, 153 (1980).
[12]G. P. Agrawal and C. Flytzanis, Phys. Rev. Lett. 44, 1058 (1980); Phys. Rev. A 24, 3173 (1981).
[13]J. A. Hermann, Opt. Commun. 37, 431 (1981).
[14]G. S. Agarwal, Opt. Commun. 35, 149 (1980).
[15]J. A. Hermann and B. V. Thompson, Opt. Lett. 7, 301 (1982).
[16]Li Fu-Li, J. A. Hermann, and J. N. Elgin, Opt. Commun. 40, 446 (1982).
[17]E. Giacobino, M. Devaud, F. Biraben, and G. Grynberg, Phys. Rev. Lett. 45, 434 (1980).
[18]C. Parigger, P. Zoller, and D. F. Walls, Opt. Commun. 44, 213 (1983).
[19]J. A. Hermann, Phys. Lett. 90A, 178 (1982); Opt. Commun. 44, 62 (1982).
[20]N. C. Kothari and T. Kobayashi, IEEE J. Quant. Electron. QE-20, No. 4 (1984).
[21]K. Shimoda and T. Shimizu, in *Progress in Quantum Electronics,* edited by J. H. Sanders and S. Stenholm (Pergamon, Oxford, 1972), Vol. 2, Part 2.
[22]N. Bloembergen and Y. R. Shen, Phys. Rev. 133, A37 (1964).
[23]L. Fuli, IEEE J. Quant. Electron. QE-19, 887 (1983).
[24]E. Lippert, W. Lüder, and F. Moll, Spectrochim. Acta 10, 858 (1959).